EJP
European Journal of Pain

ORIGINAL ARTICLE

Application of morphological characteristics of radiofrequency lesions to individual parameters of thermal rhizolysis for trigeminal neuralgia

Nicolas Massager[1,2] | Henri-Benjamin Pouleau[1] | Alexandre Jodaïtis[1] | Daniele Morelli[1]

[1]Department of Neurological Surgery, University Hospital Tivoli, La Louvière, Belgium

[2]Faculty of Medicine, Université Libre de Bruxelles, Brussels, Belgium

Correspondence
Nicolas Massager, Department of Neurological Surgery, University Hospital Tivoli, Avenue Max Buset 34, 7100 La Louvière, Belgium.
Email: nicolas.massager@chu-tivoli.be

ABSTRACT

Background: Thermic rhizolysis is a reliable therapy for pharmaco-resistant trigeminal neuralgia (TN). Temperature, duration of electrocautery and needle location can influence the efficacy and complications of the therapy.

Methods: We performed experimental thermocautery on egg white with increasing parameters of time (30–120 s) and temperature (60–95°C); we analysed the shape, size and volume of the thermic lesions produced. We developed a surgical procedure to assess peroperatively the probable thermocoagulation field and its geometric relations with the trigeminal roots and other anatomical structures of Meckel's cave, and we individually adapted the parameters of rhizolysis to optimize the results. This procedure was applied on 22 patients with TN.

Results: The volume of the lesions produced by rhizolysis on egg white had a spheroidal shape and increased linearly with the level of temperature and the time of electrocautery from 1.595 mm^3(SD 0.38) to 54.454 mm^3(SD 10.41); higher temperatures induced larger thermocoagulation fields than longer time periods. The calculated volumes measured at all levels of temperature and time were applied in vivo on the patient stereotactic planning during the thermocoagulation procedure in order to select the optimal parameters for rhizolysis. The median values used were 75°C (range 70–85°C) and 60 s (range 45–60 s). At 6-month follow-up, pain outcome was Barrow-Neurological-Institute class-I for 72.7%, IIIa for 22.7% and IIIb for 4.6%; the only complication due to rhizolysis was mild facial numbness in 13 subjects (59%) at 6-month follow-up.

Conclusion: We conclude that geometric analysis of the position of the electrode before trigeminal thermocoagulation with morphometric-related individual adaptation of treatment parameters could avoid serious injuries and optimize pain control.

Significance: We have adapted the technique of radiofrequency rhizolysis for TN. Our procedure allows individual peroperative adaptation of the parameters of thermocoagulation, according to the specific position of the electrode during rhizolysis. Preliminary results on a series of 22 patients have shown promising results.

1292 wileyonlinelibrary.com/journal/ejp *Eur J Pain*. 2022;26:1292–1303.

1 | INTRODUCTION

Radiofrequency (RF) thermocoagulation has been used clinically as a modality to treat various chronic pain syndromes since the 1950s (Mullan et al., 1963). Currently, it is one of the most frequently used neurolytic techniques for the relief of pain (Vanneste et al., 2017). High-frequency electrical current is applied adjacent to the structure of the nerve that is to be ablated, leading to ionic oscillation and frictional dissipation of the ions and electrolytes, which produces heat. RF has been demonstrated to be a more reliable and reproducible lesion production technique at a desired specific neurological location compared with electrocautery (Organ, 1976–1977).

In 1974, Sweet et al. first described a technique for generating RF lesions in the gasserian ganglion for the treatment of trigeminal neuralgia (TN) (Sweet & Wespic, 1974). Presently, percutaneous RF trigeminal rhizotomy is a well-established and effective technique for treating TN (Joffroy & Massager, 2001). The short-term pain relief is good, with a risk of recurrence mainly within 2 years after the initial RF procedure (Kanpolat et al., 2001). Accurate positioning of the rhizotomy needle in the Meckel's cave is essential to increase long-term efficacy of pain relief and reduce side effects and inadvertent complications. The procedure of RF thermocoagulation is usually performed under the guidance of fluoroscopy. More recently, some reports have been published on the use of computed tomographic or navigation guidance, or both (Arishima et al., 2016; Easwer et al., 2016; Lin et al., 2011; Thatikunta et al., 2020; Tsai et al., 2019; Weßling & Duda, 2019; Yang et al., 2010). These new systems can facilitate cannulation of the foramen ovale, especially for less experienced surgeons.

Some parameters of RF lesioning can modify the results of rhizotomy. The temperature used, the duration of RF thermocoagulation and the location of the needle tip can modify the efficacy of the therapy. Particularly, the distance between the needle and the nerve fibers that must be lesioned seems to be a crucial variable (Buijs et al., 2004; Bogduk et al., 1987). However, this parameter is often neglected, and only peroperative testing via sensitive stimulation is performed to assess correct location of the electrode's tip. Therefore, to improve the therapeutic effect of RF rhizolysis, the relative geometric position of the electrode and nerve roots into the Meckel's cave seems relevant to be studied.

On the other hand, secondary effects of RF thermocoagulation of the gasserian ganglion must also be of crucial concern. Facial numbness or dysesthesia, dry-eye syndrome or anaesthesia dolorosa are well-known troublesome complications of trigeminal rhizotomy (Joffroy & Massager, 2001). Because of proximity of important/key/vital structures around the Meckel's cave such as carotid artery or hippocampus, serious injuries have been reported (Bender & Bettegowda, 2016). So, geometric analysis of the position of the electrode during cannulation and before rhizolysis could perhaps avoid these complications.

The aim of our studies was to optimize the results of RF rhizolysis for TN by maximizing the therapeutic effect and minimizing the risks and complications of the procedure. For that purpose, we have adapted our initial procedure of RF rhizolysis by the implementation of a technique that allows an individually peroperative adaptation of the parameters of thermocoagulation to the location of the tip of the electrode into the Meckel's cave.

2 | METHODS

The present study was approved by the local Institutional Review Board and the Ethical Committee (ref. 2020/1361). Informed consent was obtained from all patients included in this study.

Statistical analysis was performed with the commercially available software GraphPad Instat® 3.10 (GraphPad©). Comparison of continuous variables was performed with the Mann–Whitney U test. The results were considered significant for $p < 0.05$.

2.1 | In vitro study

Our first study was performed in vitro and aimed to analyse the morphology of the lesion produced by RF rhizolysis using different parameters. The results of this experiment were used clinically to adapt the size of the RF lesion produced during thermocoagulation of the gasserian ganglion.

In the laboratory, we used conventional 22-gauge 100-mm Radionics RF cannulae with 5-mm active tips (Radionics, Inc.) to create the lesions. We connected the electrode to the RF generator (Universal RF system URF-3AP, Diros©) in the usual manner recommended

by the manufacturer. The electrodes were inserted into the white from 12 fresh hen's eggs placed in a rectangular glass container warmed in a water bath to 37°C. Egg white was used as model since egg white is predominantly protein and the biologic effect of conventional RF treatment is to denature protein. So, egg white seemed a suitable medium in which to examine the production of a lesion (Kwon et al., 2015; Bogduk et al., 1987). The translucency of the egg white allowed visualization of the formation of the coagulum over time. RF lesions produced in egg white were similar in geometry to those produced in both skeletal muscle and brain tissue (Moringlane et al., 1989; Vinas et al., 1992; Bogduk et al., 1987).

Bipolar RF thermocoagulation was performed as in clinical practice: the parameters of time and temperature were selected on the RF generator, then we started the lesion production and the temperature at the tip of the electrode raised rapidly (10 s max) to the desired temperature. Once the expected temperature was reached, the internal timer of the RF generator was automatically started and the RF lesioning continued for the preselected time. Then, the electrode was removed from the egg white, with the coagulum attached to it. The electrode was placed on a graph paper. The length of the coagulated white attached to the electrode was measured: the maximum size parallel to the electrode's tip and the maximum size perpendicular to it. We found, as others (Buijs et al., 2004; Bogduk et al., 1987), that the coagulum has the shape of a prolate ellipsoid of revolution (also called spheroid). So, the volume of coagulated egg white can be approximated by the formula $V = 4/3.\pi.(p/2).(q/2)^2$, where p is the max length of coagulum parallel to the electrode and q the max length of the coagulum perpendicular to the electrode.

We performed two experimental studies: the first one with increasing temperature of lesioning and constant time, and the second one with increasing time and constant temperature of lesioning. For the first study, we used a fixed time of 60 s (because it represents the standard time for this procedure) and 8 levels of temperature: 60°, 65°, 70°, 75°, 80°, 85°, 90° and 95°. For each level of temperature, we made lesions with five different electrodes. The lengths of coagulum of each electrode were measured. Then, the mean lengths of the five coagulum of each temperature level were calculated, and were used to obtain the mean volume of the 3D lesion produced by RF lesioning. For the second study, we used a fixed temperature of 75° (because it represents a commonly used level of temperature) and seven time periods: 30, 45, 60, 75, 90, 105, and 120 s. For each time interval, we made lesions with five different electrodes. The mean lengths of the five coagulum of each time interval were obtained and used to calculate the mean volume of the 3D lesion produced by RF lesioning.

2.2 | In vivo treatment procedure

Before surgery, the patients selected for treatment performed a high-resolution thin-slice stereotactic head CT and a high-resolution thin-slice stereotactic head T1- and T2-weighted MRI. For patients who had previously undergone stereotactic radiosurgery for TN, the high-resolution imaging studies of their radiosurgical treatment were retrieved and used for the current procedure.

At surgery, the patient remained under local anaesthesia with slight sedation controlled by an anaesthesiologist. The CTscanner available in the operating room (O-Arm™, Medtronic) was positioned to undergo 2D images to target the foramen ovale following the landmarks defined by Hartel (1914). After instillation of local anaesthesia into the mucosa of the cheek, we went through the intraoral mucosa with palpation and radiological guidance and we penetrate the foramen ovale with the needle. Then, we acquired 3D-scan imaging with the operating scanner (Figure S1). On the stereotactic planification software Leksell Surgiplan 11.0 (Elekta Instruments®), we retrieved these intraoperative CT images and we fused them with the preoperative CT and MR (Figure 1). The position of the tip of the needle was identified into or around the Meckel's cave on these fused images. If the position of the electrode was not adequate, the electrode was withdrawn and reinserted through the foramen ovale with a better angulation in order to reach the Meckel's cave. We performed sensory stimulation to confirm the territory of painful neuralgia and we readapted the position of the electrode if needed.

Once the electrode was located in an optimal position, the following parameters were measured on the fused images: (1) distances between the tip of the electrode and the lateral, medial, anterior, posterior, inferior and superior borders of the Meckel's cave, (2) distances between the tip of the electrode and the trigeminal nerve roots inside the Meckel's cave (Figure 2). We reported these measurements to the parameters of the spheroid lesions produced by experimental thermocoagulation during our *in vitro* study (Tables 1 and 2). We defined the optimal parameters of temperature and time to be used: we limited the parameters of time and temperature in order to avoid the risk of making a thermal lesion on structures located outside the Meckel's cave (mesiotemporal parenchyma, carotid artery, etc.), and to make an efficient RF rhizolysis on the adequate nerve root.

Then, we drew on stereotactic images a 3D-volume that corresponded to the maximal volume of lesion
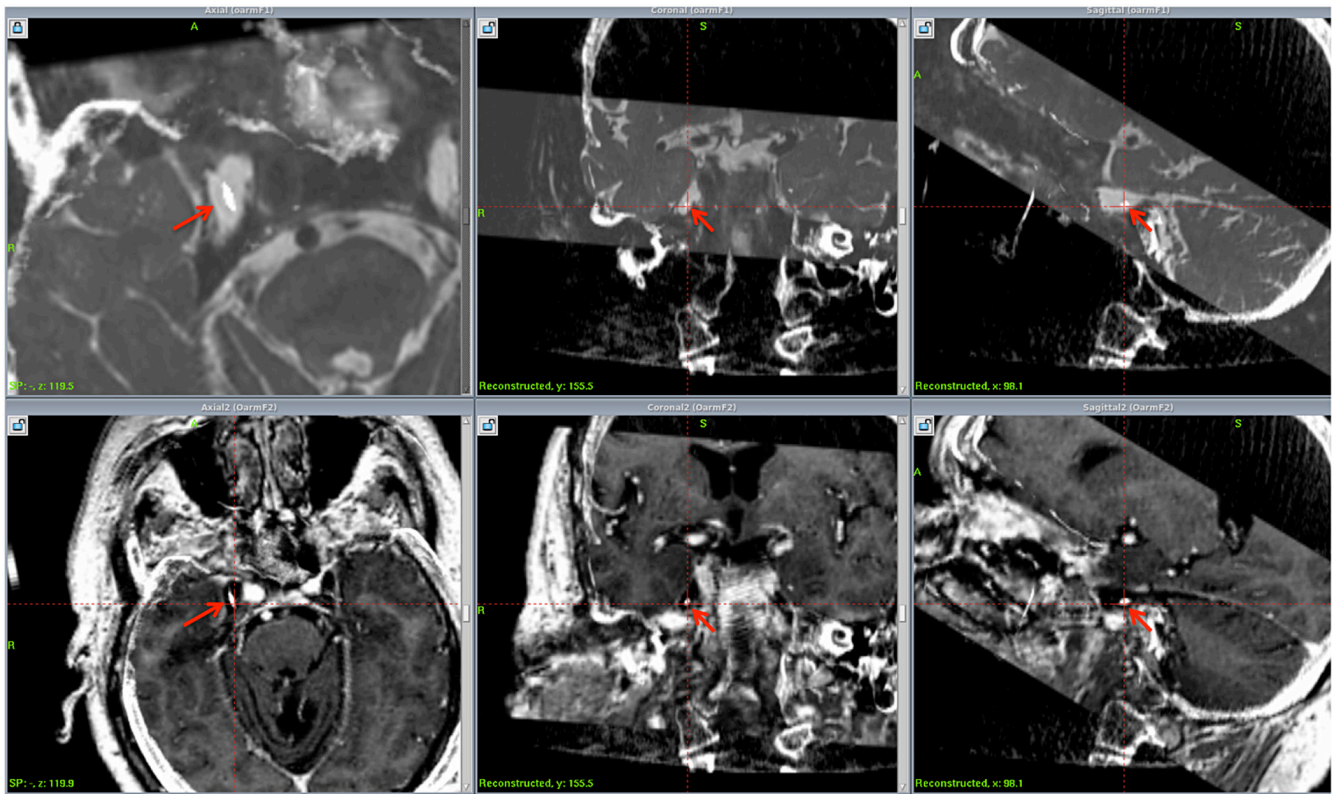
FIGURE 1 Image fusion of intraoperative CT and preoperative MRI showing the position of the tip of the electrode (red arrows) inside the Meckel's cave
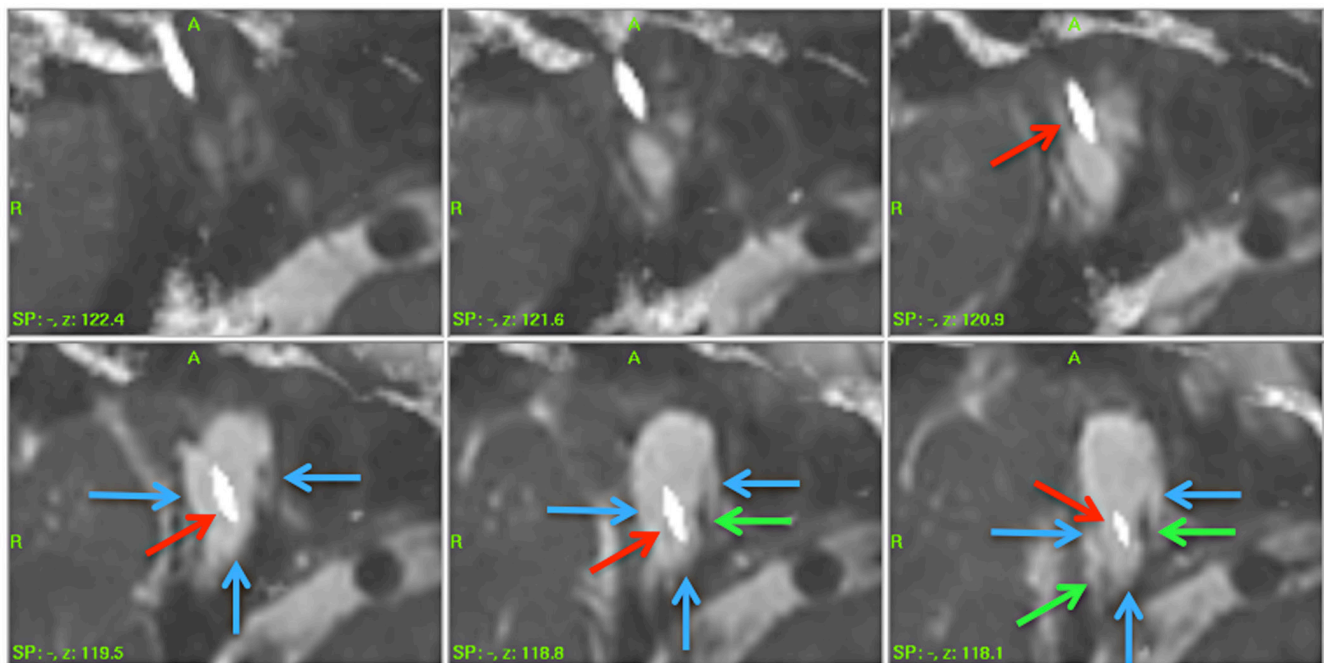
FIGURE 2 Axial image series obtained after fusion of intraoperative CT and preoperative MRI. The relation between the electrode's tip (red arrow) and the nerve roots (green arrows) and the borders of the Meckel's cave (blue arrows) can be studied

possibly taking into account the limits of the Meckel's cave and the position of the nerve roots. Next, we drew the 3D-volume of the spheroid lesion produced by experimental thermocoagulation with the parameters of time and temperature chosen. We verified by comparison between these 2 volumes that the lesion that will

TABLE 1 Mean values of *p*-distance, *q*-distance and volume of the spheroid-shaped lesion produced by RF thermocoagulation on white eggs using increasing values of temperature. The values in parenthesis refer to standard deviation

Study #1	t° levels	60°C	65°C	70°C	75°C	80°C	85°C	90°C	95°C
Time = 60 s	p (mm)	1.95 (0.33)	2.95 (0.33)	4.5 (0.31)	4.65 (0.34)	4.8 (0.27)	5.15 (0.45)	6.15 (0.42)	6.5 (0.45)
	q (mm)	1.25 (0.18)	1.45 (0.21)	2.5 (0.35)	2.6 (0.42)	2.85 (0.55)	3.25 (0.31)	3.55 (0.37)	4 (0.48)
	vol (mm³)	1.595 (0.38)	3.248 (0.58)	14.726 (4.44)	16.459 (5.74)	20.414 (9.12)	28.482 (5.67)	40.582 (8.55)	54.454 (10.41)

be produced by thermocoagulation would fit optimally (Figure 3).

Once the best parameters of thermal rhizolysis have been decided, the RF lesion was performed under brief sedation of the patient. We conduct sensory testing after thermal rhizolysis to confirm the territory of hypesthesia. The electrode was then removed, and a dressing was placed at the insertion site of the needle.

2.3 | Clinical application

This operating procedure was applied to 22 patients who suffered from intractable debilitating idiopathic TN. Patients were recruited during the period from 1 February 2020 to 31 December 2020. All patients were initially referred to the Department of Neurosurgery or the Multidisciplinary Diagnostic and Therapeutic Pain Center of the University Hospital CHU-Tivoli (La Louvière, Belgium). A preoperative evaluation was performed for all cases, including neuropsychological assessment, a brain MRI, and a medical evaluation by a neurologist.
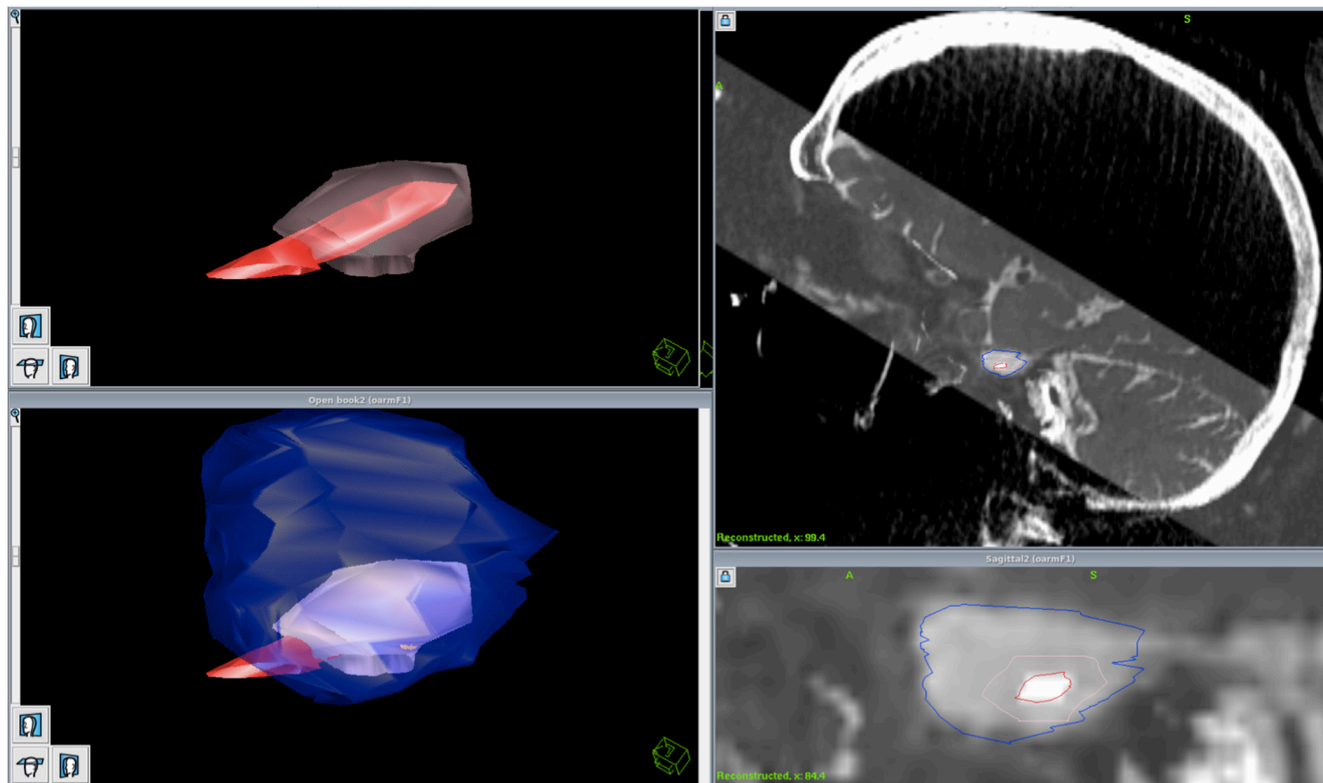
3 | RESULTS

3.1 | In vitro study

Table 1 presents the mean values of p and q distances calculated for all 8-temperature levels on the basis of the measurements recorded on the five RF lesions produced at each temperature level. At the lowest temperature level (60°C), the mean size of the lesion was 1.95 mm (SD 0.33) for *p* and 1.25 mm (SD 0.18) for *q*, and the mean calculated volume was 1.595 mm³ (SD 0.38). At the highest temperature level (95°C), the size of the lesion reached values of *p* and q more than three times the values observed at 60°C (mean 6.5 mm [SD 0.45] for *p* and mean 4.0 mm [SD 0.48] for *q*). The mean calculated volume of the lesion was 54.454 mm³ (SD 10.41).

Figure 4 presents photographs of some electrodes with coagulation of egg white obtained after RF thermocoagulation at different temperatures and a fixed time. These lesions have a spheroid shape, and their volumes are related to the parameters of RF used.

The volume of spheroid-shaped tissue involved in the RF rhizotomy has been calculated and the relation between the temperature and the volume of the lesion produced has been studied. This analysis shows that the relation between these two parameters follows a linear regression curve (Excel Software, Microsoft©) with a correlation coefficient (*r*) of 0.96983; $R^2 = 0.94057$.

TABLE 2 Mean values of *p*-distance, *q*-distance and volume of the spheroid-shaped lesion produced by RF thermocoagulation on white eggs using increasing values of time. The values in parenthesis refer to standard deviation

Study #2	Time periods	30 s	45 s	60 s	75 s	90 s	105 s	120 s
$t°=75°$	p (mm)	3.25 (0.25)	3.45 (0.37)	3.8 (0.21)	4.05 (0.37)	4.55 (0.21)	4.8 (0.27)	5.15 (0.45)
	q (mm)	1.5 (0.18)	1.55 (0.21)	1.85 (0.22)	2.05 (0.11)	2.35 (0.29)	2.65 (0.34)	2.75 (0.25)
	vol (mm^3)	3.829 (1.09)	4.340 (1.12)	6.810 (1.47)	8.912 (1.73)	13.157 (3.47)	17.649 (4.38)	20.393 (4.73)

FIGURE 3 Peroperative analysis of the optimal parameters for rhizolysis. Superior right: fusion MRI-T2 preoperative with the intraoperative CT. Inferior right: magnification of the area of the Meckel's cave on fused images, with the electrode (red contour) located inside the Meckel's cave (blue contour). Superior left: 3D reconstruction of the electrode and the area of the thermal lesion (pink volume). Inferior left: 3D reconstruction of the electrode, the area of the thermal lesion (mauve volume) and the Meckel's cave (blue volume)

Table 2 presents the mean values of *p* and *q* distances calculated for the seven studied time periods, on the basis of the measurements recorded on the five RF lesions produced for each time interval. After a 30 s period of RF lesioning, the mean *p* and *q* distances of the lesion were 3.25 mm^3 (SD 0.25) and 1.50 mm^3 (SD 0.18), respectively. The mean calculated volume was 3.829 mm^3 (SD 1.09). After a 120-s period of RF lesioning, the size of the lesion has increased to mean *p* and *q* values of 5.15 mm (SD 0.45) and 2.75 mm (SD 0.25). The mean calculated volume of the lesion after 120 s lesioning was 20.393 mm^3 (SD 4.73).

Figure 5 shows examples of electrodes with coagulation of egg white obtained after RF thermocoagulation with a fixed temperature of 75°C and various time intervals. The spheroid-shaped lesion has an increased volume in relation with the increased time of RF used. The relation found between the times used for RF-thermolesion and the volumes of the spheroid-shaped lesions observed follows a linear regression curve (Excel software, Microsoft$^©$) with a correlation coefficient (*r*) of 0.97962; $R^2 = 0.95965$.

3.2 | Clinical experience

This study included 16 women and 6 men (Table 3). Median age was 66.6y (range 42.1–83.7). Twelve patients
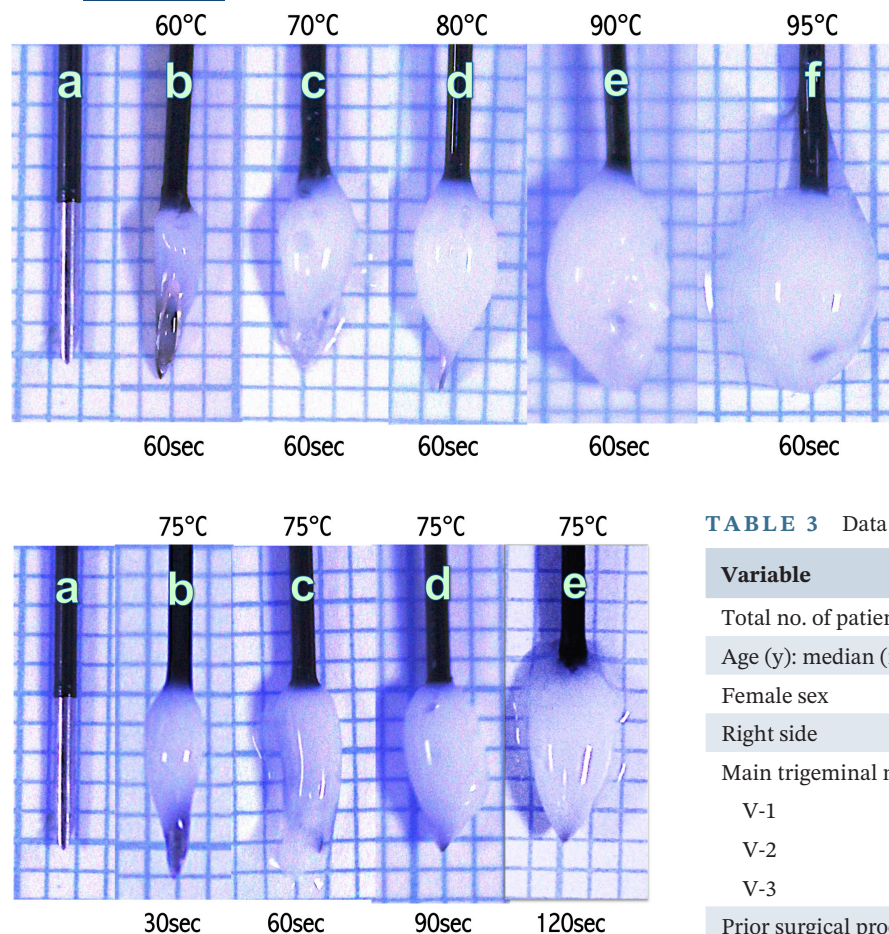
FIGURE 4 Photographs of coagulation in egg whites generated with RF currents at different levels of temperature for 60 s: (a) electrode before RF, (b) at 60°C, (c) at 70°C, (d) at 80°C, (e) at 90°C, (f) at 95°C

FIGURE 5 Photographs of coagulation in egg whites generated with RF currents at 75°C for different time periods: (a) electrode before RF, (b) during 30 s, (c) during 60s, (d) during 90 s, (e) during 120 s

TABLE 3 Data of the patients studied

Variable	Value
Total no. of patients	22
Age (y): median (range)	66.6 (42.1–83.7)
Female sex	16 (73%)
Right side	12 (55%)
Main trigeminal nerve root painful (%)	
V-1	1 (4.5)
V-2	10 (45.5)
V-3	11 (50)
Prior surgical procedure (%)	
Microvascular decompression	4 (18.2)
Radiosurgery	7 (31.8)
Percutaneous rhizolysis	6 (27.3)
Baseline distribution of pain intensity (%)	
BNI[a] class IV	13 (59.1)
BNI[a] class V	9 (40.9)
Rhizolysis: parameters	
Temperature: median (range)	75°C (70-85)
Time: median (range)	60 s (45-60)
Outcome at 6 months:	
BNI[a] class I	16 (72.7%)
BNI[a] class IIIa	5 (22.7%)
BNI[a] class IIIb	1 (4.6%)
Mild facial numbness	13 (59%)
Severe facial nerve dysfunction	0 (0%)

[a]Barrow Neurological Institute pain intensity scale (Rogers et al., 2000).

had a right TN and 10 patients had a left TN. Most of our patients had more than one nerve root affected by trigeminal seizures; the predominantly affected trigeminal nerve root was the V-1 root for 1 patient, the V-2 root for 10 patients, and the V-3 root for 11 patients.

One or several surgical procedures were done prior to the current RF treatment on 17 patients (77%). Four patients had had a previous microvascular decompression procedure, seven patients had had TN radiosurgery, and six patients had had percutaneous rhizolysis.

We have used the Barrow Neurological Institute (BNI) pain intensity scale as classification for pain assessment and pain outcome (Rogers et al., 2000). Before treatment, 13 patients had BNI class IV and nine patients had BNI class V.

The stereotactic position of the needle could have been defined precisely by the intraoperative CTscan for all patients, after co-registration of the image series to the MRI on the stereotactic planning (Figures 1 and 2). For the 22 patients, the final position of the needle was located inside the Meckel's cave. The median parameters of RF rhizolysis used were 75°C (range 70–85°C) and 60s (range 45–60 s). We tried to modify preferably the temperature first, and the time as a second option. The size of the RF-induced lesion was limited by the distance between the electrode and the border of the Meckel's cave

for 15 patients (lateral border in 13 cases, superior border in two cases) and distance between the electrode and a trigeminal nerve root of the Gasserian ganglion for seven patients (Table 4). Only one thermal lesion was performed in all cases.

All patients have been assessed at 1, 3 and 6 months after treatment. All patients had a significant improvement of pain. At the 1-month follow-up, all patients had a complete relief of the trigeminal seizures. At the 6-month follow-up, 16 patients (72.7%) had BNI class I, five patients (22.7%) had BNI class IIIa and one patient (4.6%) had BNI class IIIb. The only complication observed was mild facial numbness, which occurred for 17 patients (77%) at 1-month, and 13 patients (59%) at the 6-month control. No patient developed troublesome dysesthesia, dry-eye syndrome or anaesthesia dolorosa.

4 | DISCUSSION

In this paper, we present a surgical technique to adapt individually the parameters used for RF thermocoagulation during treatment of TN by thermal rhizolysis of the Gasserian ganglion. This procedure aimed at optimization of the functional results of the treatment and reduction of morbidity and complications.

4.1 | The egg white model

To study the size and shape of lesions produced by RF thermocoagulation, the use of fresh egg whites has already been largely validated as a suitable experimental model to study in vitro the physical effect of thermal rhizotomy (Buijs et al., 2004; Heavner et al., 2006; Kwon et al., 2015; Moringlane et al., 1989; Oh et al., 2001; Vinas et al., 1992; Bogduk et al., 1987). Egg white is essentially composed of protein. Since the biologic effect of conventional RF treatment in vivo is to denature protein, egg white is a suitable medium in which to examine in vitro the production of a lesion (Kwon et al., 2015; Bogduk et al., 1987). Moreover, the translucency of the egg white allowed visualization of the formation of the coagulum over time. Several publications have already shown that RF lesions produced in egg white were similar in geometry to those produced in skeletal muscle and in brain tissue (Moringlane et al., 1989; Vinas et al., 1992; Bogduk et al., 1987). However, as these tissues may have different physical properties than the trigeminal nerve tissue, it may be possible that the validity of this model may be reduced to predict the morphology of these lesions in such tissue. This may constitute a limitation of our experimental model.

4.2 | In vitro study

We have used fresh egg whites as a medium support to study the size and shape of the lesions produced by RF thermocoagulation. Our experiment has shown that the thermal lesion produced around the electrode's tip has the shape of a prolate ellipsoid of revolution, also called spheroid. The spheroid shape of the thermolesion we have observed corresponds to the ellipsoid or ovoid lesions described in previous studies (Moringlane et al., 1989; Oh et al., 2001; Vinas et al., 1992) in their experiment of RF lesion produced in vitro in egg whites and in vivo in the subcortical white matter of rabbits. Bogduk et al. found also that the lesion produced by RF has the shape of a spheroid (Bogduk et al., 1987).

We have found a linear relation between the volume of this spheroid lesion produced by thermocoagulation and both parameters of temperature and time. The influence of temperature and time on the size of the lesion has already been demonstrated (Moringlane et al., 1989; Pino et al., 2005; Vinas et al., 1992). However, in these articles, only the linear (Kwon et al., 2015; Moringlane et al., 1989; Vinas et al., 1992) or 2D-surfaced (Pino et al., 2005) values of the size of the thermolesion have been studied. Since the lesion produced by RF electrocautery has a tridimensional shape, it seems suitable to rather analyse the relation between the parameters of thermocoagulation with the 3D-volume of the spheroid lesion produced (Bogduk et al., 1987).

This experiment has allowed us to obtain precise measurements of the size of the thermolesion produced with different levels of temperature and time. These measures were then applied on a surgical procedure of thermocoagulation of the gasserian ganglion.

4.3 | Technical procedure of adapted RF parameters

Percutaneous radiofrequency trigeminal rhizotomy is a well-established therapy proposed for patients with TN (Kanpolat et al., 2001). In the last decade, some technical improvements have been proposed to facilitate the surgical procedure and/or optimize the results of the treatment.

The first amendment that has been proposed was to replace the traditional fluoroscopy used for cannulation of the foramen ovale by intraoperative Computerized Tomography with three-dimensional image reconstruction (Arishima et al., 2016; Easwer et al., 2016; Yang et al., 2010). CT-guidance has allowed an easier placement of the needle into the Meckel's cave through the foramen ovale, in comparison with the old technique of free-handed puncture using 2-D fluoroscopy described by

Patient	Temperature (°C)	Duration (s)	Geometrical imitation parameter
#1	80	60	Lateral border of Meckel's cave
#2	75	60	Lateral border of Meckel's cave
#3	75	60	Trigeminal root inside Meckel's cave
#4	75	60	Lateral border of Meckel's cave
#5	70	60	Lateral border of Meckel's cave
#6	75	60	Trigeminal root inside Meckel's cave
#7	85	45	Lateral border of Meckel's cave
#8	75	60	Superior border of Meckel's cave
#9	70	60	Trigeminal root inside Meckel's cave
#10	75	60	Trigeminal root inside Meckel's cave
#11	75	60	Lateral border of Meckel's cave
#12	75	60	Trigeminal root inside Meckel's cave
#13	80	60	Lateral border of Meckel's cave
#14	85	60	Lateral border of Meckel's cave
#15	80	60	Lateral border of Meckel's cave
#16	70	60	Superior border of Meckel's cave
#17	75	60	Lateral border of Meckel's cave
#18	75	60	Trigeminal root inside Meckel's cave
#19	70	60	Lateral border of Meckel's cave
#20	75	60	Lateral border of Meckel's cave
#21	80	45	Trigeminal root inside Meckel's cave
#22	80	60	Lateral border of Meckel's cave
Median	75	60	
Min	70	45	
Max	85	60	

Sweet et al (Sweet & Wespic, 1974), and is especially interesting for less experienced surgeons.

The second improvement in the technique of placement of the cannula was the use of intraoperative CT combined with integrated neuronavigation (Lin et al., 2011; Weßling & Duda, 2019). Actually, the system of cranial navigation used for brain surgery can be applied to facilitate the placement of the electrode into the Meckel's cave via neuronavigated cannulation of the foramen ovale. Some studies have shown that this procedure can be done easily and safely, even in awake patients (Lin et al., 2011; Weßling & Duda, 2019).

These new features in the procedure of RF rhizotomy of the gasserian ganglion have concerned facilitation of cannulation of the foramen ovale. More recently, another major improvement in the technique has emerged and aimed at placing the tip of the electrode at an optimal area inside the Meckel's cave (Thatikunta et al., 2020; Tsai et al., 2019). For this, a stereotactic planning system and a combination of preoperative MRI and intraoperative CT were used to provide visualization of the electrode into the Meckel's cave. The integration, coregistration and fusion of these images allow showing very clearly the position of the electrode and the borders of the Meckel's cave. With this procedure, it can be checked that the electrode can be used safely for rhizotomy, or if a repositioning of the cannulae is mandatory.

In our study, we have pushed the surgical procedure of RF thermocoagulation of the gasserian ganglion a step further. In 1974, Sweet et al. have first described a conventional procedure of thermocoagulation of the gasserian ganglion; in their paper, they proposed a standard thermal rhizolysis with fixed parameters (Sweet & Wespic, 1974). Currently, the surgeon usually defines the parameters of thermocoagulation on the basis of his personal experience. It is often difficult to know which temperature and time will be sufficient to induce a long-term sedation of the TN and to avoid complications, such as post-rhizolysis trigeminal dysfunction. We have postulated that the best way to improve the results of

this surgical procedure was to adapt individually the parameters of RF thermocoagulation.

We made a procedure to adapt for each patient during rhizolysis the parameters that must be applied to optimize the RF procedure. We studied the morphological relations between the tip of the electrode and the trigeminal nerve roots inside the Meckel's cave, as well as the limits of this cave. A simulation of the 3D area concerned by thermal cauterization is done on the stereotactic planning to choose the optimal parameters that will make an efficient rhizotomy effect on the targeted nerve root and that will avoid deleterious coagulation on the other structures located inside or outside the Meckel's cave.

4.4 | Clinical experience

We have applied our procedure to a short series of patients. The results of thermal rhizolysis in our series are promising, since the therapeutic efficacy is obtained, the rate of secondary effects is lower than usually observed and no serious complication has happened. The trigeminal seizures stopped during the first month after treatment for more than 90% of cases (Al Quliti, 2015; Gronseth et al., 2008; Kanpolat et al., 2001; Mittal & Thomas, 1986). Complications reported in the literature included (sometimes temporary) sensory loss in more than half the patients, diminished corneal reflex and eye infection in 4%–6%, anaesthesia dolorosa in 1%–4%, severe dysesthesias in 1%–6% (Al Quliti, 2015; Gronseth et al., 2008; Kanpolat et al., 2001; Mittal & Thomas, 1986). Severe complications such as oculomotor nerve paralysis, cerebrospinal fluid leakage and carotido-fistulae have also been reported (Kanpolat et al., 2001; Mittal & Thomas, 1986).

So, our initial experience suggests that the adaptation of parameters of RF by a morphological analysis of the Meckel's cave during surgery may improve the results of this procedure and minimize the risks. This experience should be continued to confirm the potential benefits of such individually adapted approach in the future. Since our preliminary experience showed that the median parameters of lesioning are the ones commonly used for classical RF, a randomized blinded trial with analysis of cost-effectiveness should be considered to estimate the benefits of our procedure.

4.5 | Limitations of the study

The study that we present here had some significant limitations. The experimental model we have used, the egg white, has been shown to reproduce the geometry of RF thermocoagulation in brain tissue, but may have some different physical properties in the trigeminal nerve tissue. The validity of this model to predict the morphology of these lesions in such tissue may consequently be reduced. Also, it is noticeable that a significant majority of our sample of TN patients had been previously treated with other surgical techniques, which may have altered the characteristics of the trigeminal nerve tissue.

Our initial clinical experience is composed of a small sample size. No control group has been evaluated as reference for comparison to the group of patients treated with our rhizolysis procedure. So, no conclusion can be drawn from the rate and type of side-effects observed in our population.

Our patients have been followed during 6 months after the rhizolysis procedure. The short-term period of follow-up represents another limitation of the scope of our results, mainly in term of trigeminal pain control. A future study designed with two arms comparing our method with the commonly used method and a longer follow-up could lead to more robust conclusions.

5 | CONCLUSIONS

With recent developments of medical imaging, we can use some of these technological advances to improve some conventional surgical therapies such as thermal rhizolysis of the gasserian ganglion used to treat TN. In this article we have reported our preliminary experience with a technique of individual adaptation of the parameters of thermocoagulation related to the position of the cauterization electrode into the Meckel's cave. The results of our treatment procedure were promising. A larger experience with this technique will show in the future if this technique is definitively associated to a better clinical outcome.

CONFLICT OF INTEREST
The authors declare no conflicts of interest.

REFERENCES
Al-Quliti, K. W. (2015). Update on neuropathic pain treatment for trigeminal neuralgia. The Pharmacological and Surgical Options. *Neurosciences*, *20*(2), 107–114. https://doi.org/10.17712/nsj.2015.2.20140501

Arishima, H., Kawajiri, S., Arai, H., Higashino, Y., Kodera, T., & Kikuta, K. I. (2016). Percutaneous glycerol rhizotomy for trigeminal neuralgia using a single-plane, flat panel detector angiography system: technical note. *Neurologia Medico-Chirurgica*, *56*, 257–263. https://doi.org/10.2176/nmc.tn.2015-0286

Bogduk, N., Macintosh, J., & Marsland, A. (1987). Technical limitations to the efficacy of radiofrequency neurotomy for spinal pain. *Journal of Neurosurgery*, *20*, 529–535. https://doi.org/10.1227/00006123-198704000-00004

Buijs, E. J., van Wijk, R. M. A. W., Geurts, J. W. M., Weeseman, R. R., Stokler, R. J., & Groen, G. G. (2004). Radiofrequency lumbar facet denervation: A comparative study of the reproducibility of lesion size after 2 current radiofrequency techniques. *Regional Anesthesia and Pain Medicine*, *29*, 400–407. https://doi.org/10.1016/j.rapm.2004.06.004

Easwer, H. V. I., Chatterjee, N., Thomas, A., Santhosh, K., Raman, K. T., & Sridhar, R. (2016). Usefulness of flat detector CT (FD-CT) with biplane fluoroscopy for complication avoidance during radiofrequency thermal rhizotomy for trigeminal neuralgia. *Journal of NeuroInterventional Surgery*, *8*, 830–838. https://doi.org/10.1136/neurintsurg-2015-011738

Gronseth, G., Cruccu, G., Alksne, J., Argoff, C., Brainin, M., Burchiel, K., Nurmikko, T., & Zakrzewska, J. M. (2008). Practice Parameter: The diagnostic evaluation and treatment of trigeminal neuralgia (an evidence-based review). Reports of the Quality Standards Subcommittee of the American Academy of Neurology and the European Federation of Neurological Societies. *Neurology*, *71*(15), 1183–1190. https://doi.org/10.1212/01/wnl.0000326598.83183.04

Hartel, F. (1914). Die behandlung der trigeminus-neuralgie mit intrakraniellen alkoholeinspritzungen. *Dehtsch Z Chir*, *126*, 429–552.

Heavner, J. E., Boswell, M. V., & Racz, G. B. (2006). A comparison of pulsed radiofrequency and continuous radiofrequency on thermocoagulation of egg white in vitro. *Pain Physician*, *9*, 135–137.

Joffroy, A., & Massager, N. (2001). Trigeminal Neuralgia: pathophysiology and treatment. *Acta Neurologica Belgica*, *101*, 20–25.

Kanpolat, Y., Savas, A., Bekar, A., & Berk, C. (2001). Percutaneous controlled radiofrequency trigeminal rhizotomy for the treatment of idiopathic trigeminal neuralgia: 25-year experience with 1600 patients. *Neurosurgery*, *48*(3), 524–534. https://doi.org/10.1097/00006123-200103000-00013

Kwon, Y. S., Lim, S. Y., Kim, J. H., Jang, J. S., Kim, C. H., Kwon, K. J., & Yon, J. H. (2015). Analysis of radiofrequency lesions in egg whites in vitro produced by application of the Tew electrode for different temperatures and times. *Pain Research and Management*, *20*(6), 316–320. https://doi.org/10.1155/2015/893136

Lin, M. H. C., Lee, M. H., Wang, T. C., Cheng, Y. K., Su, C. H., Chang, C. M., & Yang, J. T. (2011). Foramen ovale cannulation guided by intra-operative computer tomography with integrated neuronavigation for the treatment of trigeminal neuralgia. *Acta Neurochirurgica*, 1593–1599, https://doi.org/10.1007/s00701-011-1009-2

Mittal, B., & Thomas, D. G. T. (1986). Controlled thermocoagulation in trigeminal neuralgia. *Journal of Neurology, Neurosurgery and Psychiatry*, *49*(8), 932–936. https://doi.org/10.1136/jnnp.49.8.932

Moringlane, J. R., Koch, R., Schäfer, H., & Ostertag, C. B. (1989). Experimental radiofrequency (RF) coagulation with computer-based on line monitoring of temperature and power. *Acta Neurochirurgica*, *96*, 126–131. https://doi.org/10.1007/BF01456171

Mullan, S., Harper, P. V., Hekmatpanah, J., Torres, H., & Dobbin, G. (1963). Percutaneous interruption of spinal pain tracts by means of a strontium90 needle. *Journal of Neurosurgery*, *20*, 931–939. https://doi.org/10.3171/jns.1963.20.11.0931

Oh, M. Y., Hodaie, M., Kim, S. H., Alkhani, A., Lang, A. E., & Lozano, A. M. (2001). Deep brain stimulator electrodes used for lesioning: Proof of principle. *Neurosurgery*, *49*, 363–369. https://doi.org/10.1097/00006123-200108000-00018

Organ, L. W. ((1976–1977).). Electrophysiologic principles of radiofrequency lesion making. *Applied Neurophysiology*, *39*, 69–76. https://doi.org/10.1159/000102478

Pino, C. A., Hoeft, M. A., Hofsess, C., & Rathmell, J. P. (2005). Morphologic analysis of bipolar radiofrequency lesions: Implications for treatment of the sacroiliac joint. *Regional Anesthesia and Pain Medicine*, *30*, 335–338. https://doi.org/10.1016/j.rapm.2005.03.014

Rogers, C. L., Shetter, A. G., Fiedler, J. A., Smith, K. A., Han, P. P., & Speiser, B. L. (2000). Gamma Knife radiosurgery for trigeminal neuralgia: The initial experience of the Barrow Neurological Institute. *International Journal of Radiation Oncology Biology Physics*, *47*, 1013–1019. https://doi.org/10.1016/s0360-3016(00)00513-7

Sweet, W. H., & Wespic, J. G. (1974). Controlled thermocoagulation of trigeminal ganglion and rootlets for differential destruction of pain fibers. 1. Trigeminal Neuralgia. *Journal of Neurosurgery*, *40*, 143–156. https://doi.org/10.3171/jns.1974.40.2.0143

Thatikunta, M., Eaton, J., Nuru, M., & Nauta, H. J. (2020). Intraoperative CT for neuronavigation guidance and confirmation of foramen ovale cannulation for glycerol trigeminal rhizotomy: A technical report and case series. *Cureus*, *12*, e8100. https://doi.org/10.7759/cureus.8100

Tsai, P. J., Lee, M. H., Chen, K. T., Huang, W. C., Yang, J. T., & Lin, M. H. C. (2019). Foramen ovale cannulation guided by intra-operative computed tomography with magnetic resonance image fusion plays a role in improving the long-term outcome of percutaneous radiofrequency trigeminal rhizotomy. *Acta Neurochirurgica*, *161*, 1427–1434. https://doi.org/10.1007/s00701-019-03941-1

Vanneste, T., Van Lantschoot, A., Van Boxem, K., & Van Zundert, J. (2017). Pulsed radiofrequency in chronic pain. *Current Opinion in Anaesthesiology*, *30*, 1–6. https://doi.org/10.1097/ACO.0000000000000502

Vinas, F. C., Zamorano, L., Dujovny, M., Zhao, J. Z., Hodgkinson, D., Ho, K. L., & Ausman, J. I. (1992). In vivo and in vitro study of the lesions produced with a computerized radiofrequency system. *Stereotactic and Functional Neurosurgery*, *58*, 121–133. https://doi.org/10.1159/000098985

Wang, J. Y., Bender, M. T., & Bettegowda, C. (2016). Percutaneous procedures for the treatment of trigeminal neuralgia. *Neurosurgery Clinics of North America*, *27*(3), 277–295. https://doi.org/10.1016/j.nec.2016.02.005

Weßling, H., & Duda, S. (2019). ioCT-guided percutaneous radiofrequency ablation for trigeminal neuralgia: How I do it. *Acta Neurochirurgica*, *161*, 935–938. https://doi.org/10.1007/s00701-019-03859-8

Yang, J. T., Lin, M., Lee, M. H., Weng, H. H., & Liao, H. H. (2010). Percutaneous trigeminal nerve radiofrequency rhizotomy guided by computerized tomography with three-dimensional image reconstruction. *Chang Gung Medical Journal*, *33*, 679–683.

SUPPORTING INFORMATION

Additional supporting information may be found in the online version of the article at the publisher's website.